å

Design of Fuel Testing and Qualification Capsules for the Pebble Bed Advanced High Temperature Reactor

Javier Gomez, Michael Hay, James Lee, Brandon Tam
Department of Nuclear Engineering
University of California, Berkeley

Report UCBTH-10-002

May 14, 2010

ABSTRACT

Liquid fluoride salt cooled Advanced High Temperature Reactors (AHTRs) use similar TRISO fuel as is used in Modular Helium Reactors (MHRs), but have much more compact reactor cores that operate at power densities 4 to 6 times greater than in MHRs. The average coolant temperature in AHTRs is similar to MHRs (around 650°C), but AHTR fuel operates at much lower peak temperatures during normal operation (coolant outlet temperature of 700°C versus 800-950°C for MHRs) and under accident conditions (<1100°C versus <1600°C for MHRs). The low pressure, high power density, and high gas-cycle power conversion efficiency of AHTRs results in very compact primary loop systems and favorable economics. Currently, the most completely designed AHTR system is the 410-MWe Pebble Bed AHTR (PB-AHTR) developed at U.C. Berkeley. Due to high power density, this pebble fuel reaches full discharge burn up in less than one year, allowing much more rapid fuel testing and qualification than for conventional reactor fuels.

Under the Next Generation Nuclear Plant program, the United States has reestablished the complete capability to design, fabricate, irradiate, and perform post-irradiation examination of TRISO fuels. This paper provides the design basis for fuel qualification experiments at either the Advanced Test Reactor of INL or the High Flux Isotope Reactor of ORNL. These experiments will quantify the robustness of the fuel pebble design under normal operating conditions with regard to fission product attack and release. The proposed test capsules will approximate the PB-AHTR design neutron spectrum and flux while maintaining a uniform temperature at the fuel pebble surface and moderately accelerating the irradiation schedule. Neutronic and thermal analyses of the proposed fuel test capsules are presented.

CONTENTS

1.0 INTRODUCTION

The Pebble Bed – Advanced High Temperature Reactor (PB-AHTR) design implements both tristructural-isotropic (TRISO) fuel and a liquid salt primary coolant. Figure 1 below [1] illustrates several outstanding features of the design, among them passive decay heat removal [2] and the potential for process heat applications. The large heat capacity of liquid salt coolants such as flibe (Li_2BeF_4), coupled with the robustness of TRISO fuel, permits operation at a very high power density and consequently a smaller core volume. There may be significant economic and regulatory benefits associated with operating several of these modular units in lieu of a single conventional light water reactor (LWR).

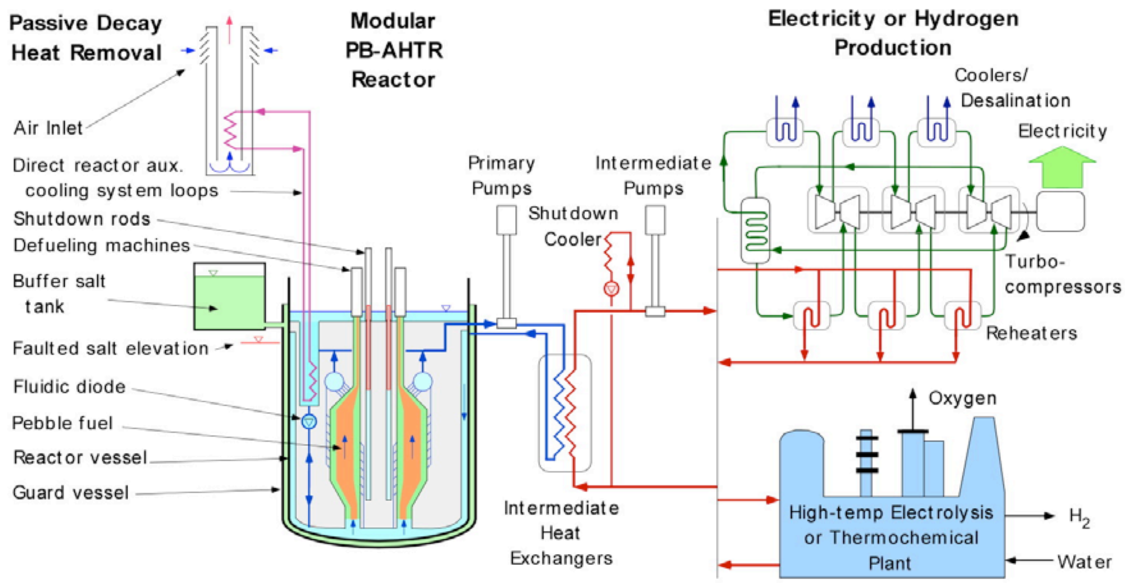

Fig. 1-1 Modular PB-AHTR schematic power cycle

The high core outlet temperatures typical of PB-AHTR operation promise thermal efficiencies (~46%) superior to otherwise comparable LWRs. The PB-AHTR is also capable of handling a number of fuel cycles, including deep burn, once-through seed blanket, and a thorium seed-blanket cycle. The robustness of TRISO fuel (implementing whichever kernel) subject to typical core fluxes and temperatures provides several hundred degrees of thermal margin to temperatures required to cause fission product release into the primary coolant. The primary coolant, which was originally developed for use with fluid-fueled reactors, has high absorption capacity for fission products. This paper offers the design basis for an experiment that will qualify proposed high burnup PB-AHTR fuels with regard to fuel particle and pebble irradiation performance.

The PB-AHTR fuel pebble consists of many TRISO fuel particles packed between a high-density graphite spherical shell and a low-density graphite center kernel. In a high burnup cycle, the TRISO fuel kernel will be composed of maximally-enriched LEU (19.9%) in the form of uranium dioxide.

TRISO-based fuel qualification studies have already been conducted for a number of advanced reactor proposals. The Advanced Gas Reactor (AGR) Fuel Development and Qualification Program [3] has been devised to improve fuel quality for plants lacking a high-pressure containment structure. One beneficiary is the Next Generation Nuclear Plant (NGNP), which has as one option a prismatic core design [4] making use of cylindrical fuel compacts composed of TRISO particles and a graphite binder. NGNP fuel compacts are being irradiated at the AGR program's main test bed, the Advanced Test Reactor (ATR) of Idaho National Laboratory [5]. The High Flux Isotope Reactor (HFIR) of Oak Ridge National Laboratory [6] is not commonly used for fuel testing, but a handful of smaller test locations are available in HFIR with exceptionally large fluxes.

The NGNP case takes advantage of the 'sweet spot' for fuel testing: not only matching the spectral features of the design reactor's expected flux, but also slightly accelerating the irradiation in the test reactor [3]. Once a reactor with a commensurate spectrum and flux has been identified, an experimental apparatus must be designed to maintain the fuel at the desired conditions inside the test reactor and subsequently facilitate data collection. The test train designs proposed here for qualifying pebble fuel are largely based on the trains designed for testing NGNP fuel compacts at ATR [7]. Among the many design considerations are flux asymmetries, temperature control, and quantifying fission product release. Because AHTR pebble fuel operates at much higher power density than NGNP fuel, it requires higher fluxes for testing and the testing can be performed much more rapidly, with irradiations taking less than one year. This is an interesting advantage for the AHTR compared to other reactor types, which typically require multiple year irradiation to test their fuel.

We reviewed the available test train designs and developed a suite of conceptual test train designs suited to qualifying pebble fuels in either ATR or HFIR. In particular, we have conducted neutronic analyses of the trains' effects on the local flux and spectrum. Maintaining the design-appropriate ratio fast-to-thermal fluxes, at whatever accelerated flux, is important to reproducing the irradiation damage expected for fuel materials. Moreover, a test train that attenuates the test reactor flux too severely is not appropriate for fuel testing. We have also conducted thermal analyses to confirm that the test trains do not significantly distort the expected radially symmetric temperature distribution within the pebble. The neutronic and thermal analyses have guided the test train design to reproduce expected fuel conditions for the duration of the testing.

Section 2 of this paper reviews the design and structural features of the fuel pebbles and their constituent TRISO fuel particles. Detailed summaries of the operating characteristics of the PB-AHTR, ATR, and HFIR will also be provided. Section 3 discusses design considerations for general components of the test trains, e.g. the gas jacket and graphite spacer material; section 4 details the design specifications particular to various test sites at the two test reactors. Section 5 lays out the neutronic analysis done for test trains designed for both ATR and HFIR, focusing on the neutron spectra available at the various test locations. Section 6 details the preliminary thermal analysis done for a prototypical test capsule design. Section 7 discusses the particular thermal features of the test capsules proposed for the various test locations.

2.0 PEBBLE AND REACTOR CHARACTERISTICS

There are advantages and disadvantages between the two test reactors available in the U.S. for PB-AHTR fuel testing. To fully irradiate the proposed pebbles to levels expected in PB-AHTR, neutron flux levels need to be in the 10^{15} $sec^{-1}cm^{-2}$ range. This eliminates the majority of operating research reactors. Reactors currently being considered as hosts to the proposed PB-AHTR fuel test train are the Advanced Test Reactor (ATR) located at the Idaho National Laboratory in Idaho Falls, ID and the High Flux Isotope Reactor (HFIR) operated by Oak Ridge National Laboratory in Oak Ridge, TN. Both reactors provide necessary flux levels and also provide the option of large test locations within the reactor. The ability to have accelerated burn up rates was also considered when narrowing the list of reactors to host the experiment. Other factors which narrowed the search to the ATR and HFIR include: ability to soften neutron flux spectrum, and provide consistent power production. The former can be achieved through the use of hafnium in the HFIR and burnable poisons can be used to provide the steady power production. Not all features are provided by both reactors, adding to the complexity of designing a proper test train.

Pebbles being used in experiment are similar to those being used in previous fuel test train experiments [7]. Our test train includes the ability to modify the composition of the fuel. One of the advantages of the PB-AHTR is the ability to accept different fuel cycles such as HEU, LEU, and also thorium for blankets.

2.1 Pebble Dimensions, Composition, and Other Properties

The fuel being tested in this test train has been designed to reach high discharge burn up levels. The spherical pebbles contain a large number of fuel particles that have many layers to allow the fuel to reach high burn up while containing all fission products within the particles. Figure 2-1 shows a scaled drawing of the multi-layered particles contained in one of these pebbles.

The fuel particle consists of a fuel kernel in the center region. The kernel is usually uranium dioxide, but thorium may also be used, which is then covered by four concentric coating layers. The layer covering the kernel is a buffer. This buffer is a porous pyrocarbon layer applied using chemical vapor deposition (CVD). Following the buffer is the inner pyrocarbon or inner low temperature isotropic (ILTI) CVD pyrocarbon layer. ILTI has a higher density than the buffer layer. The CVD layer that follows is made of silicon carbide, which is then concentrically covered with the outer pyrocarbon layer or the outer low temperature isotropic (OLTI) layer, also very dense. The size of the fuel kernel after it has been layered into what is termed a fuel particle is less than 1mm in diameter. The fuel particles then get coated with a layer of binder material and compressed together to form a fuel layer around a low density graphite sphere. The pebble is then covered with a high density graphite surface to finally create the fuel pebble, 3.0 cm (1.18’’) in diameter, which gets loaded into the reactor.

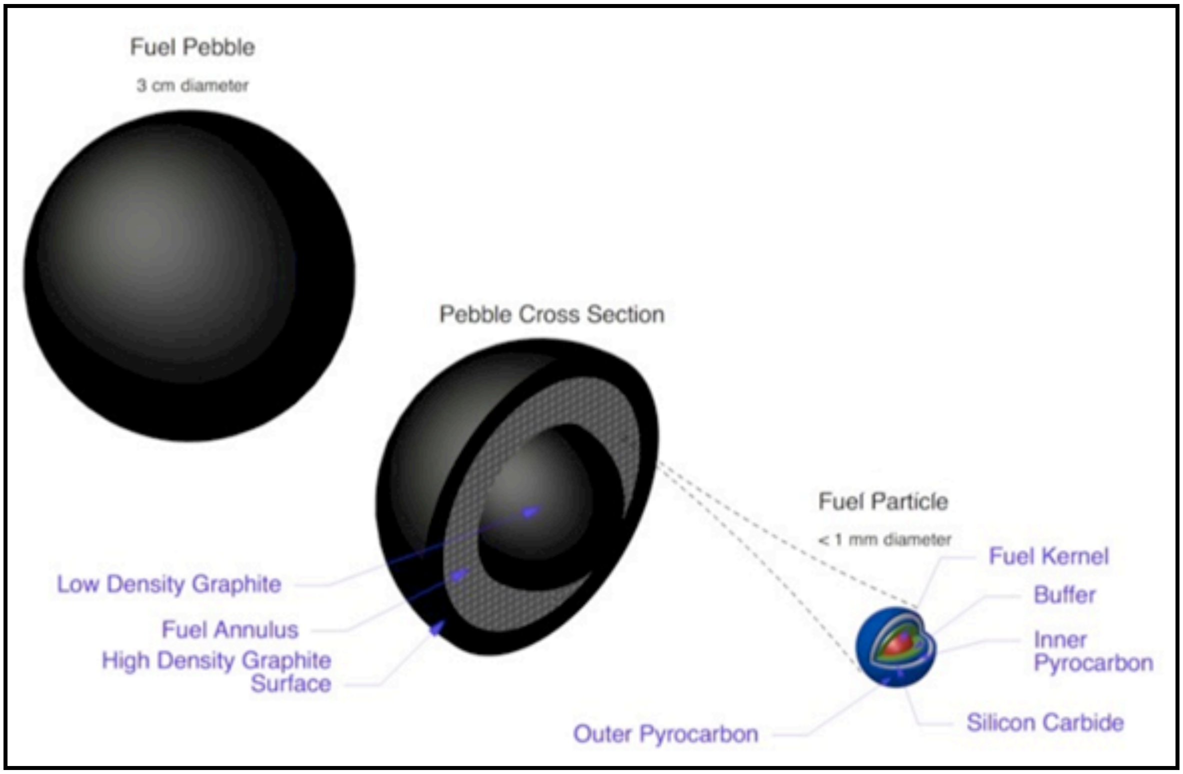

Fig. 2-1 Layering of pebble is shown. Fuel kernel may be LEU, HEU, or thorium.

A short discussion follows on the importance of each component that contributes to the composition of the fuel pebble.

The coated tristructural-isotropic (TRISO) particle ensures the fission product retention within the particle and also determines the maximum fuel temperature that can be tolerated. These determinations are based on the coated particle properties. As a result, spherical kernels are manufactured through wet chemical processes to produce a spherical shape that is ideal for supporting the stresses caused by the cocktail of fission products resulting from fuel irradiation.

The buffer layer that concentrically surrounds the kernel is highly porous pyrocarbon with approximately 50% of the theoretical density of pyrocarbon. It provides a space for the gaseous fission products to fill, which relieves some of the stresses from pressure build up on the kernel, and it is flexible enough to allow for kernel swelling as a result of irradiation.

The ILTI pyrocarbon layer follows after the buffer. This layer is the first to protect from fission product pressures. Not only does it serve as a barrier against pressure, protecting the outside graphite matrix, but because of its high density, it acts as a nearly impenetrable wall for fission products derived from the kernel.

The silicon carbide (SiC) provides the most robust and fundamental basis for safe operation of reactors using pebble fuel. It remains under a compressive stress as provided by the ILTI and OLTI layers, which shrink under irradiation. This SiC layer prevents cesium, strontium, and (at temperatures below 1100°C) silver from exiting the coated particle and entering the graphite matrix. The ILTI and OLTI layers lose their ability to contain these fission products at high temperatures. If fission products make it to the graphite matrix, they can then transport to the reactor coolant.

The next layer, that has already been discussed because it sandwiches the SiC, is the OLTI layer. Its two main functions are to protect the SiC layer from possible damage during the processes after the kernel layering. Also it reduces the tensile stress in the SiC layer by providing pre-stress on the outside of the SiC. The OLTI layer has the function of maintaining the integrity of the spherical fuel particle by protecting the most important safety feature of the layering process. It has been shown that cracked layers in the coating or spherical deviations in the final fuel particle product can lead to increase risk of particle failure.

To prevent cracking or damage from fuel particles coming into contact with each other, the fuel particles are covered in very fine ground matrix graphite. This overcoating, as it is referred to, is the beginning of the next stage, the fuel sphere.

It is important to note a few of the benefits of using graphite material for the fuel encasings. First, the graphite adds dimensional stability, maintaining the integrity of the spherical shape under fast neutron irradiation. Second, it can be relatively easy to press the matrix graphite into desired density. But the most important functions of the graphite are to protect the coated particles from mechanical damage, provide a heat conduction path between the coated particle and the reactor coolant, and to moderate neutrons for the fuel inside the coatings. The final diameter of the fuel pebble is 3.0 cm.

An advantage of the PB-AHTR is the ability to accommodate various fuel cycles. Table 2-1 is provided by Tommy Cisneros of UC Berkeley [11] but it shows all of the considered fuels to be used and their mechanical properties. Values missing have either not been set or determined.

2.2 PB-AHTR

The technology used for the liquid-salt cooled reactor (PB-AHTR) allows for a nominal thermal power output of 900 MW_{th} and with an efficiency of 46%. It can produce a net electrical power output of 410 MWe. But also very important is the fact that the PB-AHTR supports advanced fuel cycle programs. This stems from the fact that the PB-AHTR can be thought of as a composite, formed from the different technologies of a variety of reactor types. For example, it uses the TRISO particles pebble fuels from the PBMR and other MHRs that are helium cooled. It shares the advanced safety codes used for Light Water Reactors such as the AP-1000. The PB-AHTR also boasts a pool-configuration and DRACS to remove decay heat is a passive manner derived from sodium fast reactors. But key to this reactor are the liquid salt pumps and corrosion resistant alloys used in the Molten Salt Reactors. We explore the different cycle options in our research. The reactor technology has the ability to use the deep burn, once-through seed-blanket, and thorium seed-blanket fuel cycles. Deep burn cycles are beneficial since they allow for the burning of plutonium to very high burn up levels. Once-through seed-blanket cycles will use low enriched-uranium with a thorium blanket to reduce the amount of fuel needed and also reduce expenses and waste produced. The last fuel cycle supported by the PB-AHTR is that of the thorium seed-blanket fuel cycle, which produces lower amounts of plutonium and other long lived transuranics. It is important to note that the PB-AHTR can operate at core power densities of 20-30 MW_{th} and that it is the liquid salt coolant with its high heat capacity that provides these benefits.

Table 2-1 Table shows mechanical properties for various proposed fuels to be used in proposed design test train.

PB-AHTR fuels and corresponding values			
Fuel type	LEU	LWR-	Thorium
Pebble type	seed	seed	blanket
Enrichment	19.9%	n/a	0%
Pebble diameter (cm)	3.0	3.0	3.0
Inner kernel radius (cm)	0.712	n/a	0.77
Outer shell thickness (cm)	0.2	0.2	0.2
Total mass heavy metal (g)	2.8	n/a	6.37
Design discharge burn up	21.4%	n/a	20.6%
Total energy generated (MW_ehr)	6.37	n/a	13.0
Used fuel volume (m^3/GW_eyr) (2)	23.5	n/a	15.9
Number fuel particles per pebble	13380	n/a	6455
Average pebble density (g/cm^3) (3)	1.78	1.78	1.84
Average pebble power (kW_t)	1.74	0.70?	0.20
Time to reach full burn up (yr)	0.91	n/a	33.7
Kernel density (g/cm^3)	10.5	n/a	9.7
Graphite binder density (g/cm^3)	1.602	n/a	1.2
Graphite shell density (g/cm^3)	1.74	n/a	1.74
Particle kernel diameter (μm)	350	n/a	600
Particle kernel density (g/cm^3)	n/a	n/a	n/a
Particle outside diameter (μm)	760	n/a	952
Particle packing density	40 %	n/a	40 %

1) PB-AHTR thermal efficiency 46%, PBMR thermal efficiency 43%.
2) A typical LWR would produce 19.4 m^3/GWeyr of used fuel (1100-MWe PWR, 18-month refueling outage cycle, 193 assemblies, 1/3 removed, stored in 1.70-m diameter, 4.60-m long, 21-assembly canisters).
3) Graphite blanket pebbles have a density of 1.74 g/cm^3.

2.3 ATR

The Advanced Test Reactor at Idaho National Laboratory can be used to test fuel and document materials behavior under and after irradiation. This test reactor is a 250 MW_{th} pressurized LWR which is divided into five main regions of different levels of neutron fluxes, and which consists of nine flux traps. According to INL' s ATR User Guide, "there are an additional 68 irradiation positions in the reactor core reflector and an additional 34 low flux irradiation positions in the tanks outside the reactor core reflector tank" [5]. This large number of positions allows a wide variety of experiments to be conducted concurrently. Furthermore, experiments can be cooled using the ATR's coolant, or experiments may be designed with their own test loops in which flow rates, pressures, temperatures, and neutron flux may be specified. This research project explored the third option available within the ATR. The third option is to design a test train with capsule and instruments to monitor the behavior of the fuel and background conditions. This sort of experiments is termed Instrument Lead Experiment. It involves a capsule with lead tubes attached for carrying instrument wires and temperature control gases in and out of the reactor vessel. These types of experiments are more complex than static capsules because they have equipment coming in and out of the test capsules. But these allow for control of temperature for specific zones as gases acting as insulators/conductors can be varied from outside the reactor. Drawbacks of such Instrument Lead Experiments include higher costs and more time to install and remove the individual experiments.

The ATR's maximum thermal neutron flux, 1.0×10^{15} n/cm^2-sec, at full 250MW_{th} power, initially posed issues for our desired burn up rates. Issues arose because the reactor is rarely operates at full power and we need similar fluxes to hope for comparable irradiation results. The following figure is a list of specifications provided by INL for its ATR. Values provided here were used to simulate temperature distributions and burn up rates.

Figure 2-2 and Table 2-2 show the ATR's different flux traps and other available locations for irradiation and expected neutron flux levels in the ATR , respectively. Both, Figure 2-2 and Table 2-2, are provided by an ATR User Guide provided by INL. In addition, the flux traps shown in Figure 2-3 are ideal for the designed test train as one of these operating at full power, provides necessary flux levels to mimic PB-AHTR irradiation effects. Table 2-2 lists the thermal and fast neutron fluxes of the ATR's various locations within the reactor, each at the core mid-plane with the ATR operating at 100MW_{th}. It is important to note that neutron flux within the reactor varies not only varies from site to site, but it also varies along the vertical length of a test position.

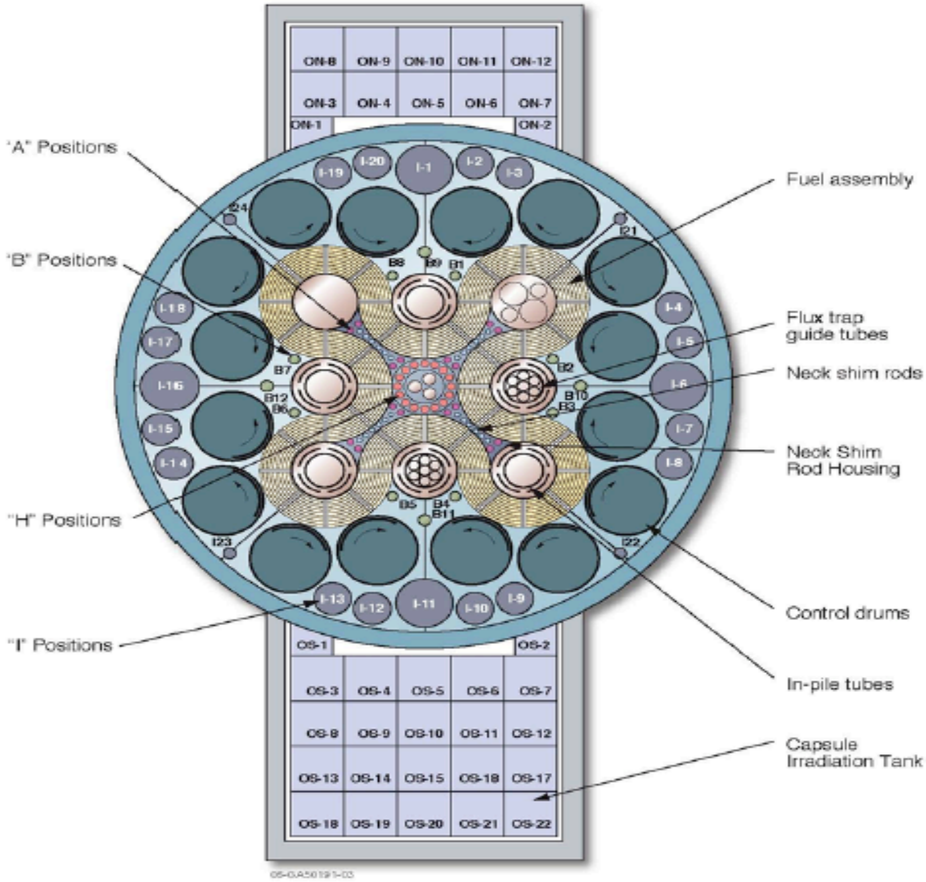

Fig. 2-2 ATR view from the top shows the four flux traps and other test positions.

Table 2-2 Neutron flux is listed per position available in ATR.

Positions	**Diameter (in.)[a]**	**Thermal Flux (n/cm^2-s)[b]**	**Fast Flux (E>1MeV) (n/cm^2-s)**
Northwest and Northeast Flux	5.250	$4.4x10^{14}$	$2.2x10^{14}$
Other Flux	3.000[c]	$4.4x10^{14}$	$9.7x10^{13}$
A-Positions			
(A-1 – A-8)	1.590	$1.9x10^{14}$	$1.7x10^{14}$
(A-9 – A-12)	0.659	$2.0x10^{14}$	$2.3x10^{14}$
(A-13 – A-16)	0.500	$2.0x10^{14}$	$2.3x10^{14}$
B-Positions			
(B-1 – B-8)[e]	0.875	$2.5x10^{14}$	$8.1x10^{13}$
(B-9 – B-12)	1.500	$1.1x10^{14}$	$1.6x10^{13}$
H-Positions			
(H-1 – H-16)	.625	$1.9x10^{14}$	$1.7x10^{14}$
I-Positions			
Large(4)	5.000	$1.7x10^{13}$	$1.3x10^{12}$
Medium(16)	3.500	$3.4x10^{13}$	$1.3x10^{12}$
Small(4)	1.500	$8.4x10^{13}$	$3.2x10^{12}$
Outer Tank Position			
ON-4	Var[d]	$4.3x10^{12}$	$1.2x10^{11}$
ON-5	Var[d]	$3.8x10^{12}$	$1.1x10^{11}$
ON-9	Var[d]	$1.7x10^{12}$	$3.9x10^{10}$
OS-5	Var[d]	$3.5x10^{12}$	$1.0x10^{11}$
OS-7	Var[d]	$3.2x10^{12}$	$1.1x10^{11}$
OS-10	Var[d]	$1.3x10^{12}$	$3.4x10^{10}$
OS-15	Var[d]	$5.5x10^{11}$	$1.2x10^{10}$
OS-20	Var[d]	$2.5x10^{11}$	$3.5x10^{9}$

a. Position diameter. Capsule diameter must be smaller
b. Average speed 2,200 m/s
c. Current east, center, and south flux trap configurations contain seven guide tubes with inside diameters of 0.694 in
d. Variable; can be either .875, 1.312, or 3.000 in.
e. B-7 is the location of the Hydraulic Shuttle Irradiation System

An important specification which dictated the design of our proposed test train is the variety in test position dimensions supported by the ATR. This variation can be seen from Table 2-2. Available test positions, according to the ATR User Guide, range in diameter size from 1.67 cm (0.659’’) to 13.34 cm (5.25’’). This variation allowed the research group to examine a variety of different pebble arrangements in the proposed design.

To compliment the table above, listed properties of the ATR are shown below on Table 2-3.

Table 2-3 Properties of ATR provided by ATR User Guide.

Reactor:	
Thermal power	250 MW_{th}[a]
Power density	1.0 MW/L
Maximum thermal neutron flux	$1.0x10^{15}$ n/cm^2-sec[b]
Maximum fast flux	$5.0x10^{14}$ n/cm^2-sec[b]
Number of flux traps	9
Number of experiment positions	68[c]
Core:	
Number of fuel assemblies	40
Active length of assemblies	4 feet
Number of fuel plates per assembly	19
Uranium-235 content of an assembly	1,075 g
Total core load	43 kg[d]
Coolant:	
Design pressure	2.7 MPa (390 psig)
Design temperature	115°C (240°F)
Reactor Coolant:	
Light water maximum coolant flow rate	3.09 m^3/s (49,000 gpm)
Coolant temperature (operating)	<52°C (125 °F) inlet, 71°C (160 °F) outlet
a. Maximum design power. ATR is seldom operated above 110 MW_{th} b. Parameters are based on the full 250 MW_{th} power level and will be proportionally reduced for lower reactor power levels. c. Only 66 of these are available for irradiations. d. Total U-235 always less due to burn-up	

To cap off the ATR discussion, the procedure for irradiating targets, whether it be materials or fuel elements, goes as follows: Targets are inserted into the ATR inside "experiment assemblies." The components of these assemblies are the targets, the capsule, and the basket. The capsule serves to provide a boundary to contain the target material and isolate it from the reactor primary coolant. The capsule is designed with an internal annulus generally filled with an inert gas such as helium or argon. The basket serves as the housing of the capsule and is designed to fit properly with the irradiation position in the reactor.

2.4 HFIR

The High Flux Isotope Reactor located in Oak Ridge National Lab, is also being considered as a possible host to our experiment test train. HFIR is a 100 MW_{th} LWR, which uses uranium-235 as fuel and is beryllium-reflected. It is more commonly known as an isotope producer, but it is equipped for research locations inside the reactor and outside through beam tubes which direct neutrons. The locations for irradiation experiments go as follows: "(1) four horizontal beam tubes, which originate in the beryllium reflector; (2) the hydraulic tube facility, located in the very high flux region of the flux trap, which allows for insertion and removal of irradiation samples while the reactor is operating; (3) thirty target positions in the flux trap, which normally contain transuranium production rods but which can be used for the irradiation of other experiments (two are instrumented target positions provided by a recent modification); (4) six peripheral target positions located at the outer edge of the flux trap; (5) numerous vertical irradiation facilities of various sizes located throughout the beryllium reflector; (6) two pneumatic tube facilities in the beryllium reflector, which allow for insertion and removal of irradiation samples while the reactor is operating for activation analysis; and (7) four slant access facilities, called "engineering facilities," located adjacent to the outer edge of the beryllium reflector. In addition, spent fuel assemblies are used for gamma irradiation in the gamma irradiation facility in the reactor pool" [9]. These descriptions have been provided by Oak Ridge National Laboratory and Figure 2-3, also provided by ORNL, better depicts the irradiation position layout inside HFIR.

In accordance with the design test train, eight larger diameter irradiation positions located in the removable beryllium (RB) locations have been identified as prospective locations within the reactor to conduct our experiment in. The RB locations are near the control region and therefore sufficient neutron flux levels can be expected to meet PB-AHTR levels. Furthermore, these locations within the reactor allow for either instrumented or non-instrumented experiments, which are highly desired in our test train. The instrumented design "facility", as it is referred to by ORNL, will allow" the instrumented capsule design to employ sweep or cooling gases as necessary…and accommodate access tubes through penetrations in the upper shroud flange and through special penetrations in the pressure vessel hatch" [9]. The RB positions can be seen in blue on Figure 2-3.

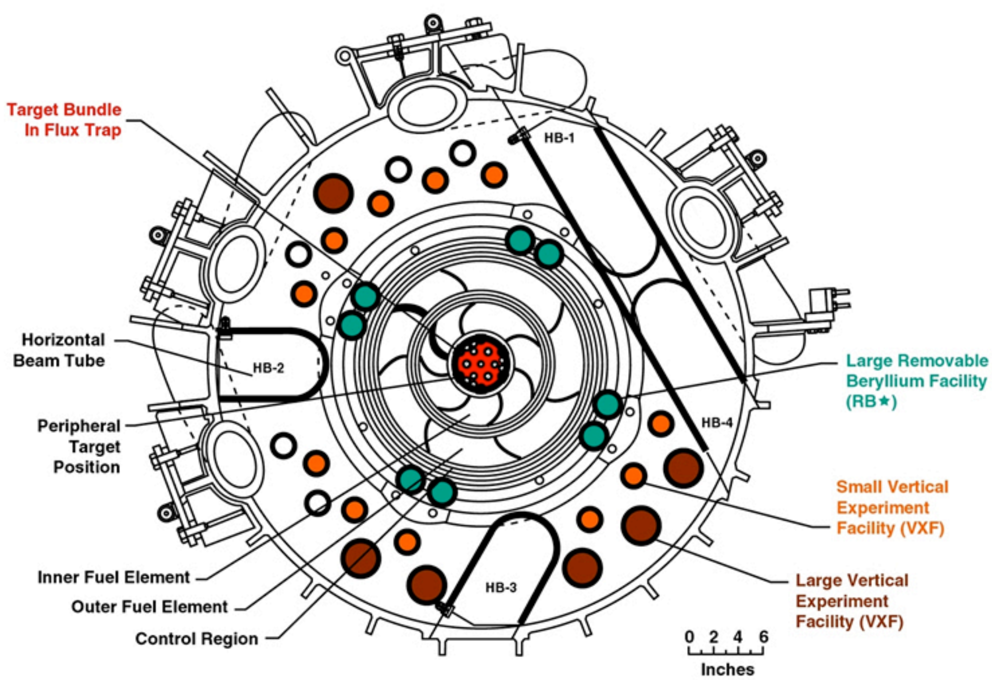

Fig. 2-3 HFIR experiment locations for irradiation as seen from the top.

Also important to our heat transfer modeling is the total flow rate of approximately 16,000 gpm, of which 13,000 gpm are expected to pass through the fuel region and the remaining 3,000 gpm pass through experiments and the remaining regions. Inlet coolant temperatures is 120°F (49°C) and corresponding exit temperature is 156°F (69°C) with a pressure drop through the core of approximately 110 psi (7.58 x 10^5 Pa) [9].

Furthermore, ORNL has also provided a figure of expected neutron flux. The neutron flux graph, Figure 2-4, is for $100MW_{th}$ operation of the reactor, or full power. According to ORNL, the flux can be scaled linearly with power, so for the operation of the reactor at 85 MW_{th}, we can expect neutron flux levels to be scaled back by 15%.

Typical radial neutron flux distributions in the core's horizontal midplane at 100MWth

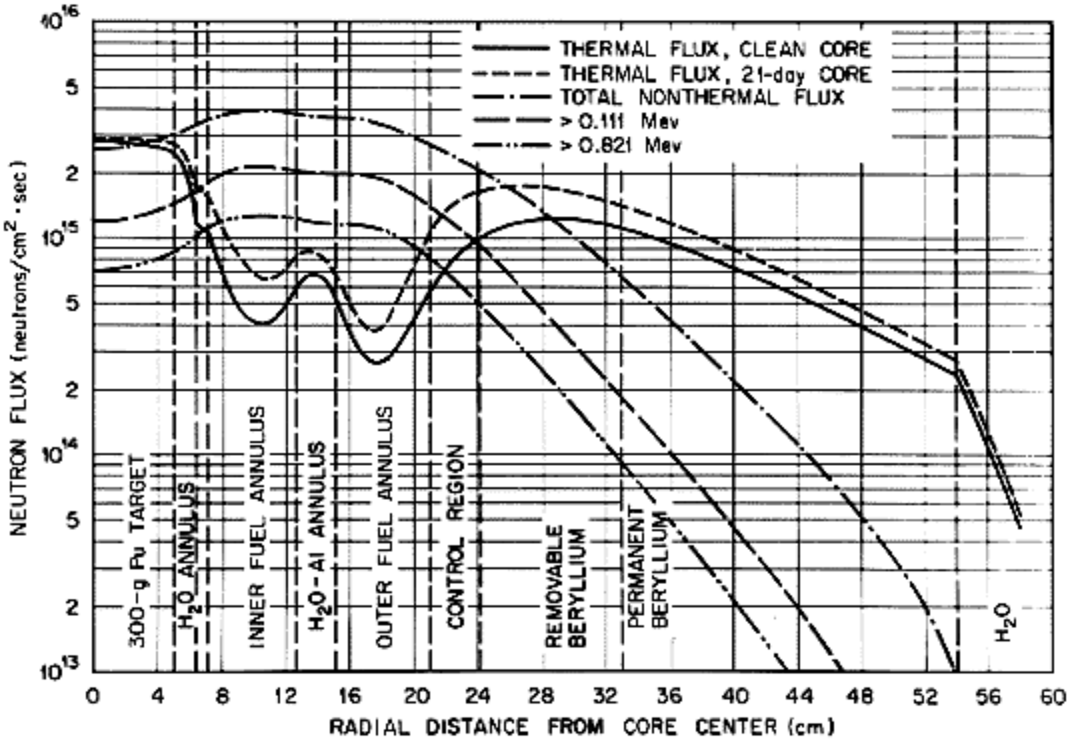

Fig 2-4 Graph shows the unperturbed fluxes of HFIR's horizontal midplane at 100MW. Neutron flux varies linearly with power levels. For 85 MW_{th}, reduce neutron flux values to 85%.

3.0 TEST CAPSULE COMPONENTS

Two test reactors and three test locations lead to several capsule designs. While each design is unique, they all share common components. Fig. 3-1 shows all of these primary components.

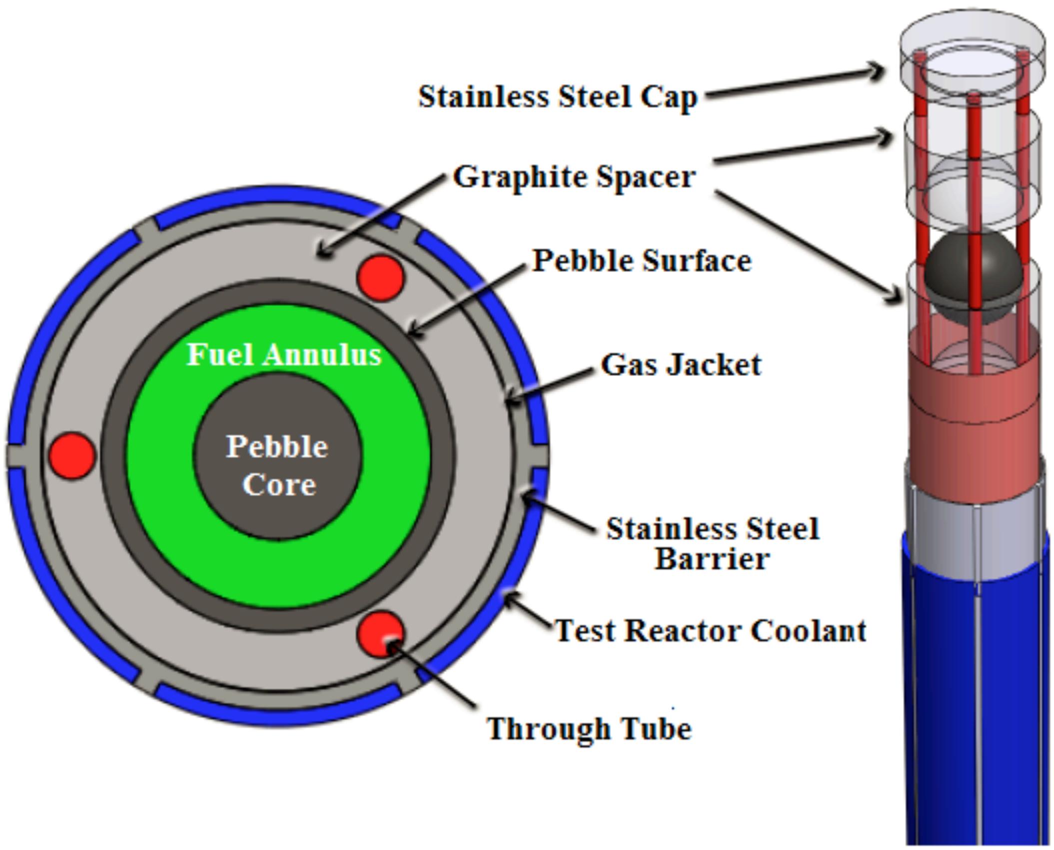

Fig. 3-1 Cross sectional and exploded view of a test capsule

The stainless steel barrier allows the pebbles to be cooled while not being in contact with the coolant. The gas jacket allows for temperature control and the graphite spacers hold the pebbles and conduct heat from the pebbles to the capsule wall. Through tubes contain the thermocouples and gas lines for the multiple test capsules in the test train and the stainless steel caps keep the coolant from entering the test capsule at the top or bottom. The following sections discuss the nonspecific test reactor capsule design in more detail.

3.1 Graphite Spacer

The graphite spacers have three main purposes: to hold the pebbles, establish a uniform gas jacket thickness, and conduct heat to maintain a uniform and controlled pebble surface temperature. A more uniform pebble surface temperature is achieved by spacing the pebbles farther apart. This aspect of the graphite spacer design is discussed in more detail in the COMSOL analysis section of the report. Two types of graphite spacers are used to hold the pebbles and are shown in Fig. 3-2. The intermediate spacers have a hemisphere machined into the top and bottom of the spacer while the end spacers are only machined on one side. All of the pebbles' surfaces are covered by using several intermediate spacers and two end spacers. While the spacers shown in Fig. 3-2 only have one pebble position per face, designs for some of the larger test locations have multiple positions.

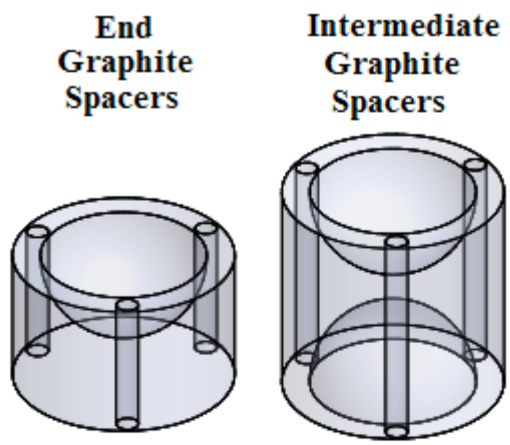

Fig. 3-2 Graphite spacer examples

As the graphite spacers form the inner radius of the gas jacket used for temperature control, they must be accurately centered in the test capsule to insure a uniform gas jacket thickness. The spacers are aligned using the stainless steel barrier, through tubes, and capsule caps and the specifics of this alignment are discussed in section 3.3.

3.2 Gas Jacket

The gas jacket is a thin layer of gas between the stainless steel barrier and graphite spacer. The insulating gas jacket not only provides a means to test pebbles operating at different powers at the same temperature, but also insulates the pebbles so they can reach their normal PB-AHTR operating temperatures.

The temperature of the capsule is primarily determined by the pebble power, gas jacket thickness, graphite thermal conductivity, and gas thermal conductivity. For a given pebble power, the maximum temperature the capsule can reach is dictated by the gas jacket thickness which cannot be altered during irradiation. Temperature control during irradiation is achieved by varying the thermal conductivity of the gas jacket. By utilizing a gas mixture composed of a gas with a relatively high conductivity and one with a relatively low conductivity, He and Ne respectively, a wide range of temperatures can be reached for a given gas layer thickness.

The results of a simple cylindrical geometry 2d calculation shown in Fig 3-3, were used for scoping calculations to choose the gas thickness for the initial designs. In this calculation a graphite spacer thickness of 4 mm, stainless steel thickness of 1.5 mm, and a test reactor coolant thickness, velocity, and temperature of 1 mm, 2 m/s, and 52 °C, respectively were used. The fuel pebble was approximated as a cylinder with a height and radius equal to that of the actual pebble.

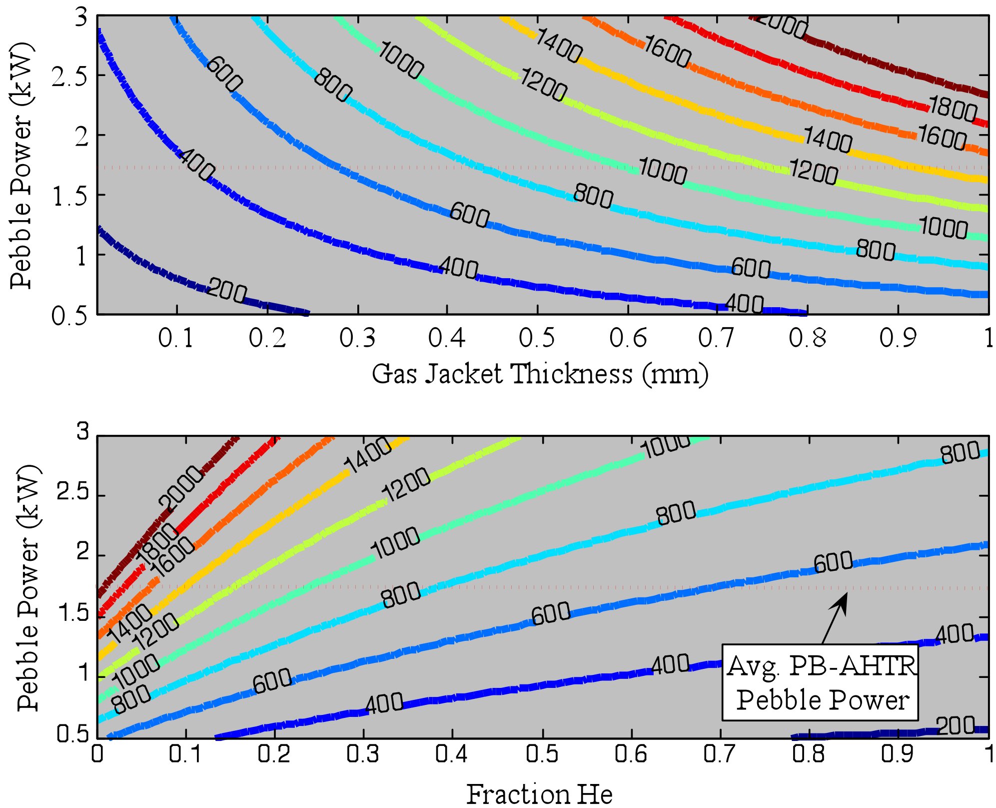

Fig 3-3 Top: Calculated pebble surface temperatures for a range of powers and gas jacket thicknesses. Bottom: Pebble surface temperatures varying the gas composition in a 0.2 mm jacket.

These results led to an initial gas jacket design thickness of 0.1 mm for capsules in which the pebble power is expected to be 1.74 kW, the average PB-AHTR pebble power. While the temperature in the capsule can be decreased by approximately 2.5 times by changing gas composition from 100% Ne to 100% He, the rapidly increasing temperature with increasing gas jacket thickness reinforces the need for a uniform gas jacket thickness.

3.3 Stainless Steel Barrier, Through Tubes, and Caps

The stainless steel barrier, through tubes, and caps insure a uniform gas jacket thickness while performing other functions. The stainless steel barrier forms the outer most layer of the capsule. It isolates the pebbles, graphite spacers and gas jacket from the test reactor coolant while also aligning the capsule in the test location. Based off previous fuel qualification test capsules designs, a stainless steel thickness of 1.5 mm was used for all of the designs[3, 8]. The mechanical properties of the stainless steel barrier were not evaluated.

Each of the through tubes in a capsule have an outer diameter of 4 to 6 mm and contain the gas lines and thermocouples for the other capsules in the test train

The necessary uniform gas jacket thickness is achieved by using the capsule caps and through tubes to center the graphite spacer. Fitting the through tubes into a capsule's stainless steel cap, which is centered in the stainless steel barrier, centers the graphite spacers, as shown in Fig. 3-5.

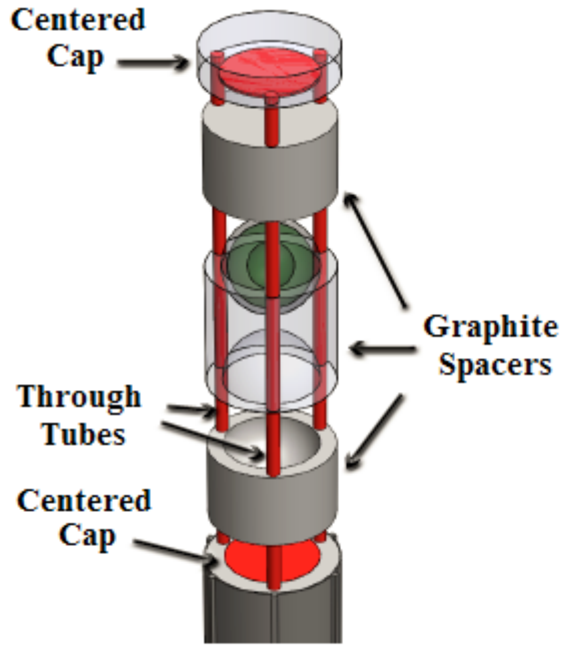

Fig. 3-5 Exploded view of a test capsule illustrating the centered graphite spacers

Depending on the test location, the stainless steel caps have heights of 5 to 10 mm and various radii. In addition to having openings for the through tubes, the caps have a layer of insulating gas to achieve a more uniform axial temperature profile.

While not included in the SolidWorks and COMSOL models, the final cap design would include a means for the thermocouples and gas lines to enter the capsule. While thermocouples and gas lines for adjacent capsules would first enter the cap and then pass through the through tubes, those used within the capsule would penetrate the cap and enter the graphite spacers. To do this, the caps would probably be a hollow cylinder with a removable top.

4.0 TEST REACTOR SPECIFIC CAPSULE DESIGNS

As the radii, lengths, and flux profiles vary between the ATR and HFIR test locations, specific test capsule designs had to be developed for both. The following sections describe the reactor specific test capsule designs.

4.1 HFIR Test Capsule Design

As discussed in section 2.4, the test location in HFIR has a small radius and length relative to PB-AHTR pebbles. Due to the small radius of the test location, only one pebble can be at each graphite spacer face. The HFIR axial flux profile limits the number of pebbles that can be irradiated in each capsule to two, as discussed in the neutronics and Comsol analysis sections of the report. These two restrictions lead to a two pebbles per capsule design shown in Fig. 4-1.

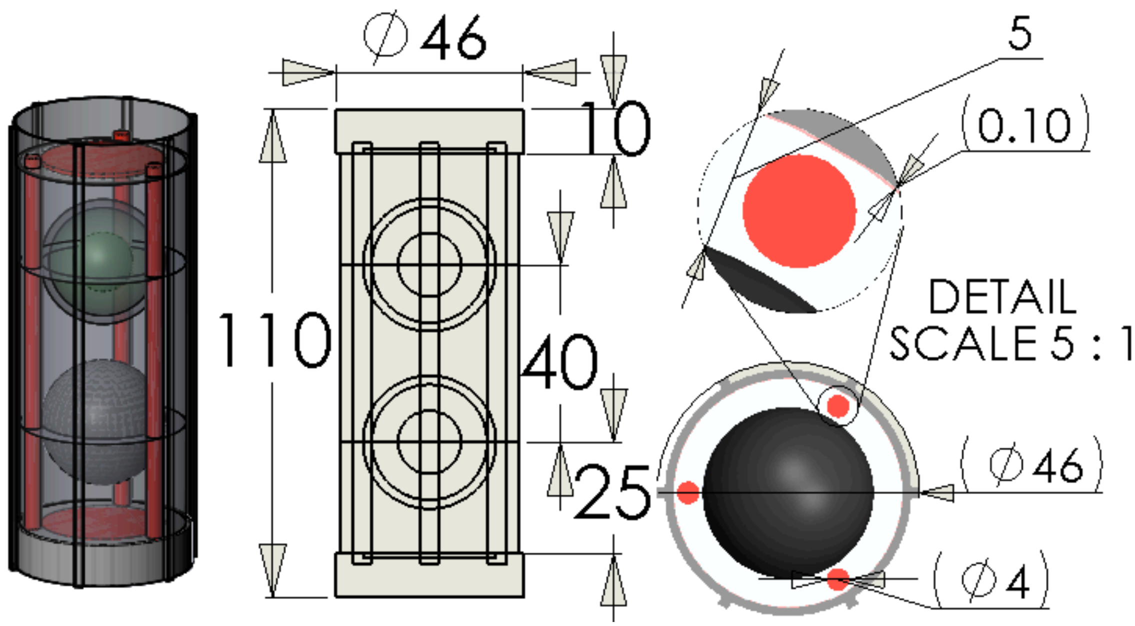

Fig. 4-1 Test capsule design for HFIR, measurements in mm

An aspect unique to the HFIR capsule design is that it has the same radius as the test location while the ATR capsule designs reserve a couple of millimeters to provide space for hardware to connect multiple test capsules.

4.2 ATR 3'' Flux Trap Test Capsule Design

The simplest design for the 3'' flux trap is the HFIR design with more pebbles per capsule. As discussed in the neutronics and Comsol analysis sections of the report, four pebbles can be contained in the ATR test capsules. A four pebble per capsule version of the HFIR design is shown in Fig. 4-2.

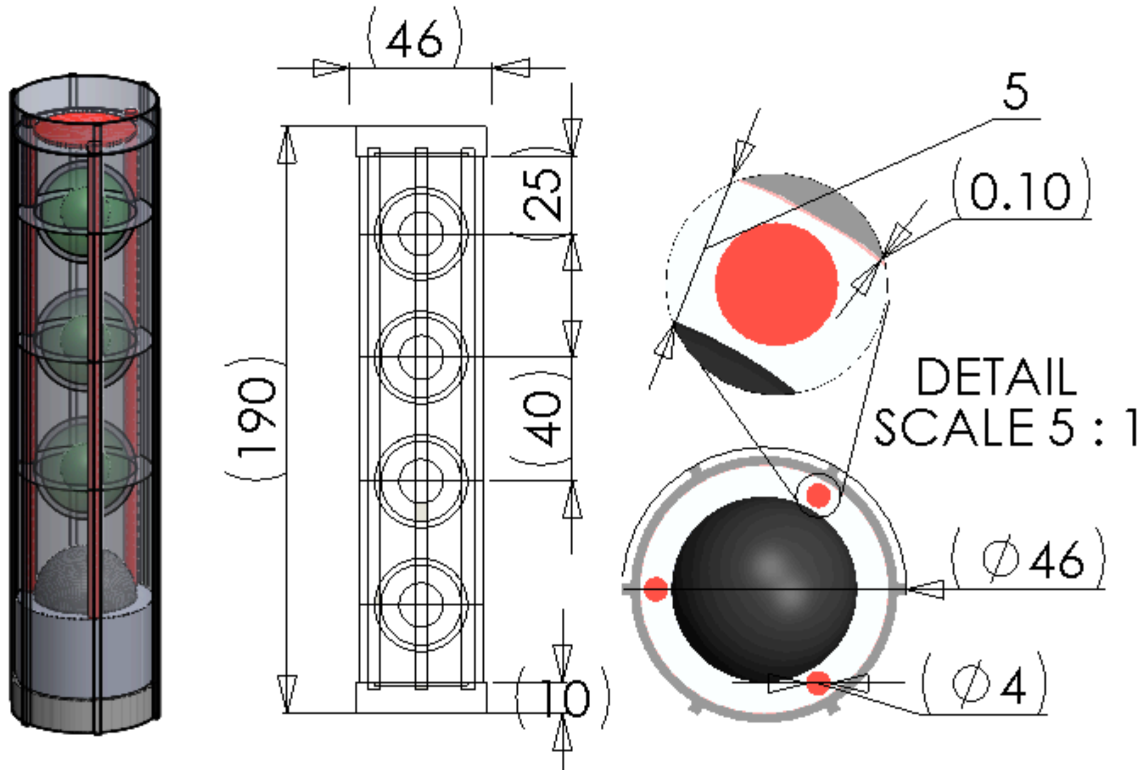

Fig. 4-2 The ATR axial flux profile allows for larger test capsules, measurements in mm figure caption provides a brief description of the figure, in this case a comparison of the cross sections of two different types of heat exchangers.

While the capsule design for HFIR could be used in the ATR, a capsule specifically designed for the 3'' flux trap can utilize the space more effectively. This can be achieved by placing three pebbles at each graphite spacer face. The resulting capsule contains twelve pebbles as shown in Fig 4-3.

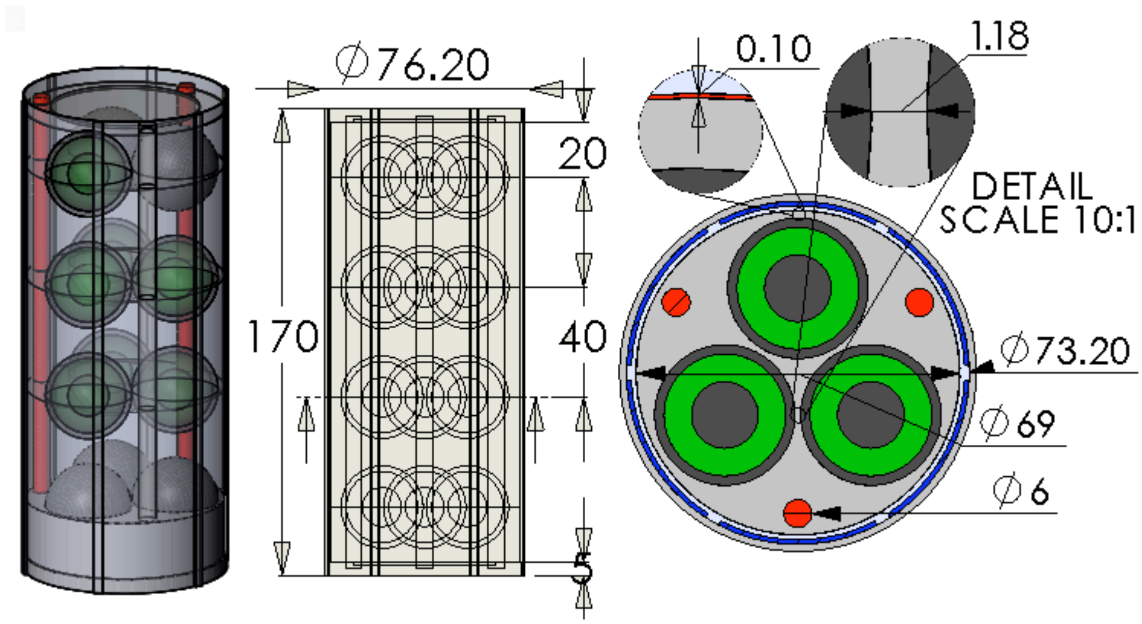

Fig. 4-3 Three pebble test capsule design for ATR, measurements in mm

Placing multiple pebbles on each graphite spacer face allows more pebbles to be tested but also makes the temperature profile in the graphite spacer more irregular. Due to high centerline temperature in the capsule, the non-uniform pebble surface temperature in this design outweighs the benefits of testing more pebbles.

The effectiveness at lowering the centerline temperature by placing a high thermal conductivity sheet of metal between the pebbles, as shown in Fig. 4-4, is investigated in the COMSOL analysis section of the report.

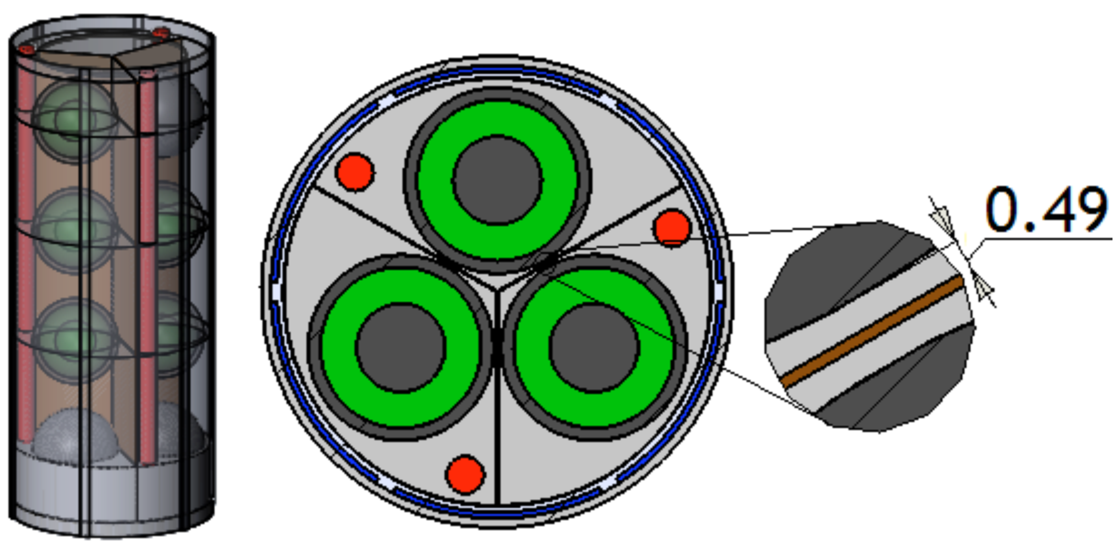

Fig. 4-4 Cross section showing the metal strip used to lower the temperature between pebbles, measurements in mm

4.3 ATR 5.25'' Test Capsule Design

The 5.25'' flux trap in the ATR allows for multiple pebbles to be placed at each graphite spacer face without being in close proximity. Initial 2D COMSOL results indicated that a 10 mm spacing is needed between the pebbles to establish uniform pebble surface temperature. By placing five pebbles on a spacer face a spacing of 15.2 mm is achieved. As this spacing was more than adequate, a five pebble per graphite face design, Fig. 4-5, was chosen for the 5.25'' flux trap. This design contains twenty pebbles per capsule.

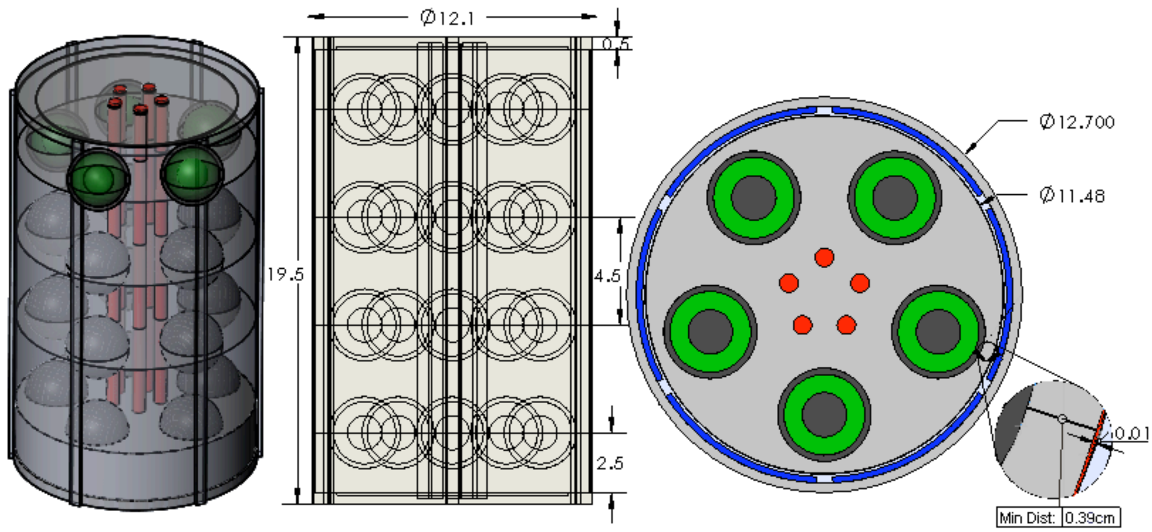

Fig. 4-5 Test capsule design for the 5.25'' flux trap, measurements in cm

While a sixth pebble could fit in the graphite spacer, it would effectively be completely shielded from the reactor thermal neutron flux. Instead of a pebble, the through tubes were placed in the center of the capsule. Five through tubes were chosen primarily for symmetry. The two additional through tubes may prove useful as more thermocouples would most likely be needed to monitor to the temperature of twenty pebbles.

As discussed in the COMSOL™ section, the spacing was adequate for the axial temperature profile to be uniform, but high temperatures in the center of the graphite spacer lead to a non-uniform pebble surface temperature. To lower the temperature in the center of the graphite spacer a channel for coolant to flow through was placed in the center of the capsule. The resulting annular capsule is shown in Fig. 4-6

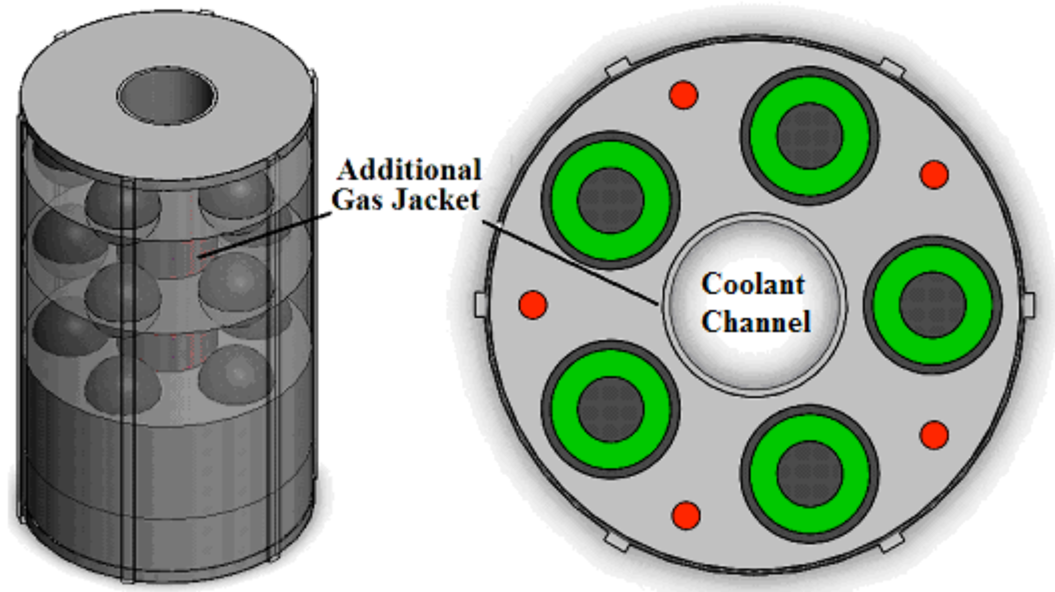

Fig. 4-4 Coolant flowing through the center of the capsule allows for a more uniform temperature profile

Along with a channel to allow coolant to flow through the center of the capsule, an additional gas jacket is needed to raise the centerline temperature and is shown in Fig. 4-6. The stainless steel barrier previously discussed could be modified to form the new barrier in the center of the capsule or a stainless steel pole could run the length of the test train and be used to connect the capsules.

5.0 NEUTRONICS

As the heat source in the test capsules is the pebbles, coupling the capsule thermal design and capsule neutronic design is essential. While Monte Carlo calculations would give more accurate numbers, simple hand calculations were used to understand the first order effects of the test capsule on the reactor neutron flux.

The primary goal of the capsule neutronics design is to insure the pebbles will be subjected to a flux similar to that in the PB-AHTR and that they reach full burn-up. For fuel pebbles in the PB-AHTR the neutron flux for the average power pebble, 1.74 kW, is 8.04×10^{14} n/cm^2 s. 18.8% of the flux is fast, >.1 MeV for the fuel pebbles and 17.3% for the blanket. As such, the capsules are designed to expose the fuel pebbles to a thermal neutron flux of 6.53×10^{14} or greater wherever possible. The ratio of thermal to fast flux the pebbles are exposed to should also be similar to that of the PB-AHTR. At the 3'' and 5'' flux traps in the ATR the fast flux, >.025 eV, is approximately 22% and 50% of the total flux, respectively. In HFIR the fast flux, >.111 MeV is approximately 19% of the total flux. Hafnium can be used to soften the neutron spectrum in the 5'' flux trap but was not considered in this report.

5.1 Calculation Assumptions

Each component of the test capsule reduces the neutron flux the pebbles are exposed to. Table 1 lists the thermal neutron cross sections of the isotopes that make up the components.

Table 5-1 Microscopic thermal neutron cross sections for test capsule

Test Capsule Component	**Isotope**	**ϱ (g/cm^3)**	**σ^{th} (b)**
Graphite Spacer	C(natural)	2.23	4.95
Gas Jacket	^{4}He	1.78×10^{-4}	.86
Stainless Steel Barrier	^{56}Fe	7.85	14.77
Stainless Steel Barrier	^{52}Cr	7.85	3.74

To calculate the neutron attenuation, several assumptions were made. The stainless steel was assumed to be 10 at% Cr, and the gas jacket was ignored due to is relatively small neutron cross section and small, 0.1-mm thickness. Fig. 5-1 shows reduction in flux in a capsule with a 0.15-cm stainless steel barrier and 0.4-cm graphite spacer.

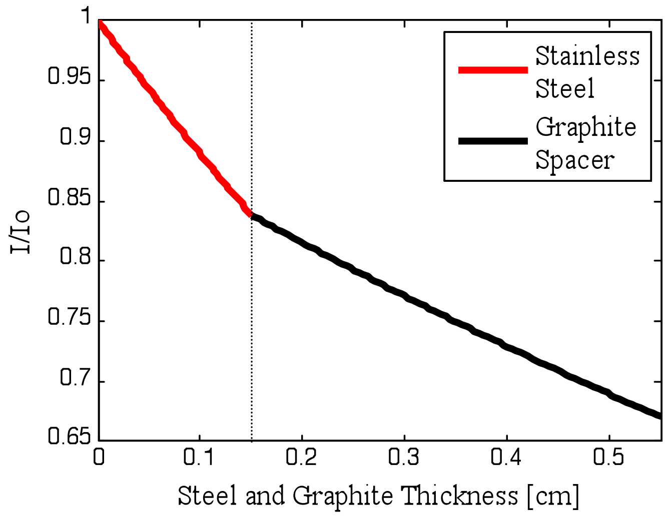

Fig. 5-1 The reduction in flux for a typical capsule's stainless steel and graphite spacer thicknesses

To calculate the pebble power several more assumptions had to be made. First the pebble power was assumed to scale linearly from 1.74 kW at a flux of 6.63×10^{14} n/cm^2 s. Second, for the multiple pebble per graphite face designs, the test location flux was assumed to be the same on the test capsule from all directions. As the flux traps are partially surrounded by the fuel assembly, as shown in Fig 5-2, this assumption is not completely unreasonable. Thirdly, the flux attenuation is calculated for a 1.5 mm thick stainless steel barrier and the minimum thickness of graphite between the barrier and pebble surface. Assumptions two and three together applied to the designs in chapter 2 result in pebbles at each graphite spacer face, i.e. the same axial position, being at the same power. Finally, the different values for fast flux >.025 eV, >.111 MeV, >.1 MeV, for the ATR, HFIR, and PB-AHTR, respectively, was not taken into account. Instead all of the calculations are done assuming the thermal flux given was .025 eV.

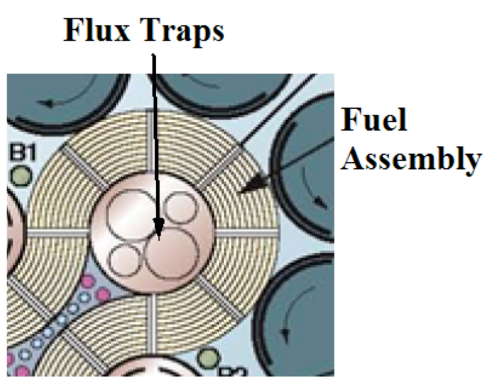

Fig 5-2 The ATR fuel assembly encompasses the flux traps

Second order polynomials were fit to the available axial flux profiles [9-10] in order to calculate the pebble power at different axial positions in the test reactors. The resulting axial flux profiles are shown below in Fig. 5-3.

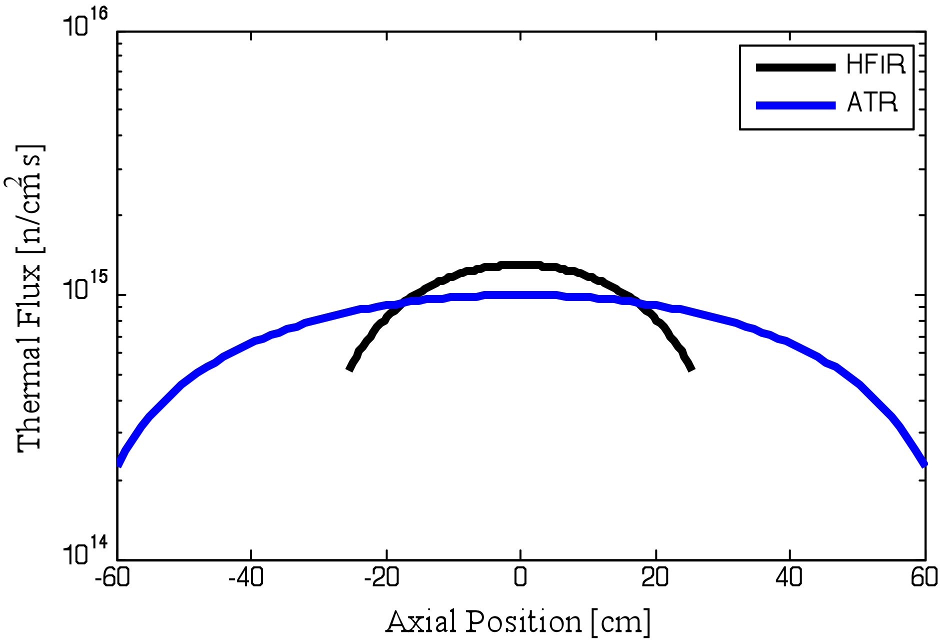

Fig 5-3 Test reactor axial flux profiles

While the shape of the profiles were determined by the fit, the magnitude is based off the assumptions that HFIR is operating at 85 MW and that one of the fuel lobes in the ATR is at full power, 50 MW.

5.2 HFIR Test Capsule Neutronics

Incorporating all of the assumptions, Fig. 5-4 shows the calculated pebble powers for the HFIR test capsules.

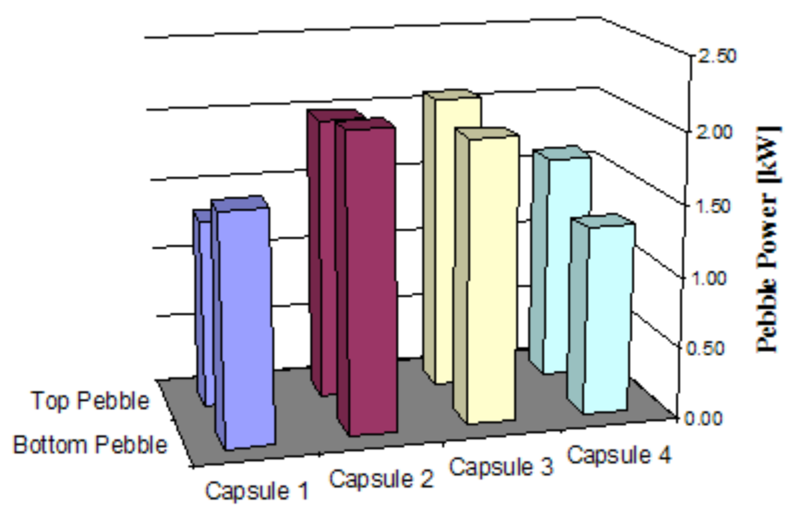

Fig. 5-4 Calculated pebbles' powers in HFIR, the active core mid-plane is between capsule 2 and 3

Due to the large axial gradient in flux relative to the size of the fuel pebbles, only two pebbles were placed in each capsule. Four of the resulting capsules, discussed in section 4.1, fit in the RB* test location. Even though only two pebbles are contained in each capsule, the pebbles in the first and last capsules vary in power substantially. Furthermore, the pebbles in capsules 2 and 3 are at much higher powers than those in 2 and 4 which would need much longer irradiation times. Fig. 5-5 shows how these effects are reduced if three, rather than four, capsules are used.

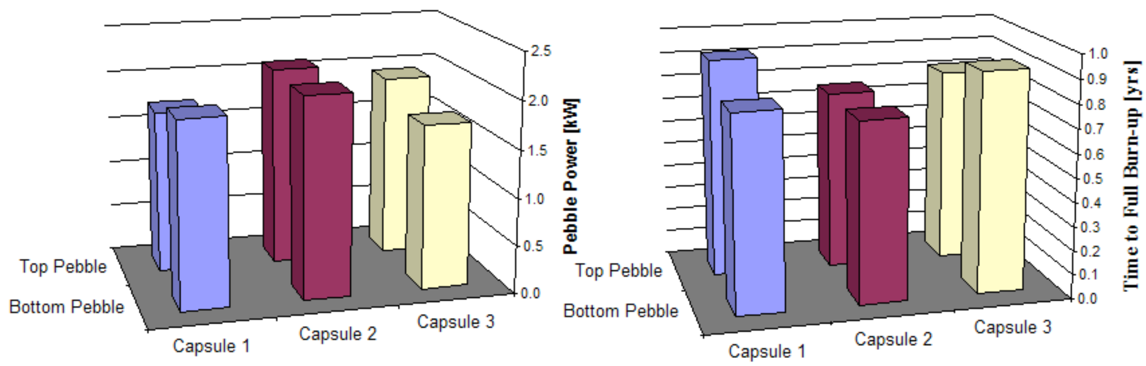

Fig. 5-5 Calculated pebbles' power and time to full burn-up in HFIR, capsule 2 is centered on the active core mid-plane

With three capsules in HFIR, the pebbles in the first and last capsule vary in power by 0.2 kW and the time to full burn-up varies by 0.2 yrs between capsules. Neutron absorbers could be placed in capsule 2, which would otherwise reach full burn-up in .75 years, so that all of the pebbles would take approximately 0.9 years to reach full burn-up. This length of time is very close to the fuel pebbles time to full burn-up in the PB-AHTR of 0.91 years. This is a very rapid fuel irradiation time compared to conventional LWR, MHR, and SFR fuels, and is a clear development advantage for the PB-AHTR.

5.3 ATR Test Capsule Neutronics

The ATR's longer active core length of approximately 120 cm reduces the axial gradient in flux. As such, four pebbles were placed in each of the capsules. Five of the resulting capsules, discussed in sections 4.2 and 4.3, fit into the ATR flux traps, as shown in Fig 5-6.

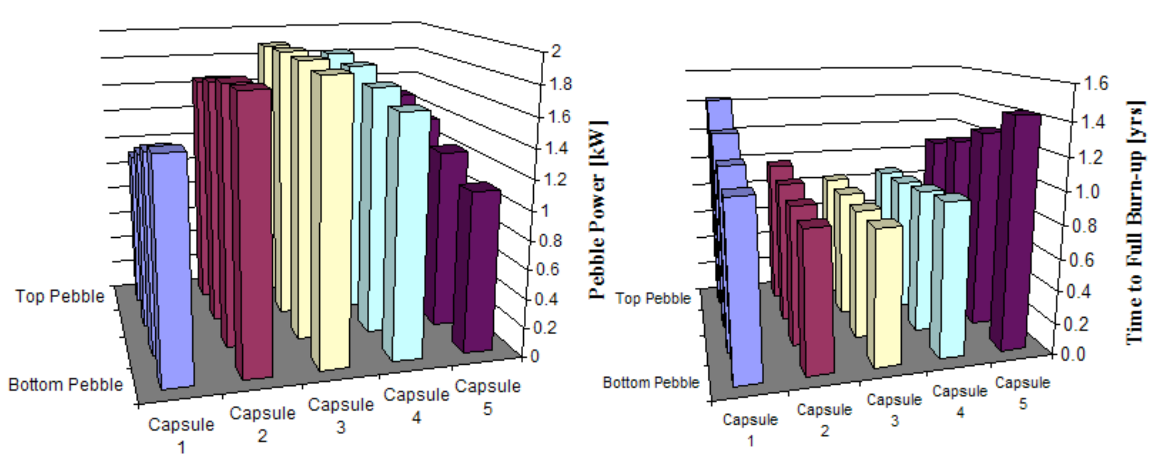

Fig. 5-6 Calculated pebbles' power and time to full burn-up in the ATR, capsule 3 is centered on the active core mid-plane

As was the case in HFIR, the first and last capsules' pebbles vary in power significantly and are at much lower powers than the other capsules. By only using capsules 2, 3, and 4 the maximum difference in pebble power in a capsule is 0.15 kW. By using neutron absorbers in capsule 3, which would otherwise reach full burn-up in 0.83 years, all of the pebbles would take approximately 0.9 years to reach full burn-up.

6.0 TEST CAPSULE THERMAL ANALYSIS

Since the test capsules will be placed in both test reactors to simulate the PB-AHTR operating environment, a high temperature environment, it is essential to have an understanding of the test capsules temperature distribution to prevent capsules from reaching undesirable high temperature. A complete thermal analysis would provide suggestive locations to place thermal couples which will be used to monitor the capsule temperature. Additionally, it gives information on the maximum number of pebbles that can be place inside a single capsule.

To approach the problem, thermal analysis is first done on geometrical simplified 2D models on the y-z plane. The following section will discuss the 2D y-z plane thermal analysis done on a simplified ATR3" 1 pebble capsule design on COMSOL™ in detail.

6.1 2D Axial Symmetric Thermal Analysis

The number of pebbles placement in the capsule is limited by the geometry of the reactor test location; consequently the number of pebbles that can be placed inside a single capsule is narrowed down to the three model shows in Fig. 1 – 3 pebbles, 4 pebbles and 5 pebbles. This section will explore thermal analysis of the simplified ATR3" 1 pebble capsule design. The thermal analysis is done on the y-z plane which will give suggestive maximum number of pebbles that can be placed inside a single capsule. Through this primitive 2D analysis, couple assumption has been made to simply the problem: 1) All pebbles have identical power generation regardless of its position; 2) the Helium is stationary inside the gas jacket; 3) Gas jackets assume to cover the top and bottom of the test capsule, as a result boundary condition of capsules located on the bottom of the test train are chosen to be thermal insulated rather than the inlet coolant temperature; and 4) simplified design geometry. All constants used in the primitive thermal analysis are defined on the table below.

Fig. 6-1 shows the temperature distribution of three different models of the ATR3" 1 pebble capsule with Helium. By making the assumption that the capsule is place in between two other capsules, the boundary condition of the graphite region of each capsule in Fig. 6-1 is set to be thermal insulated. Comparing three models, the temperature distribution of the 5 pebbles model is undesirable: temperature between pebbles is too high with maximum temperature reaching 886°C. Since the maximum temperature of PB-AHTR is around 1100°C, the 5 pebble model is not recommended. Both thermal analysis on 4 pebbles and 3 pebbles models demonstrates decent temperature distribution. However, in order to maximize pebble tested in a single capsule, the 4 pebbles model is preferred over the 3 pebbles model.

To improve the thermal analysis preciseness on each model, singular circle pebble geometry is replaced by concentric circles to represent three different layers of the pebble: 1) low-density graphite shell; 2) fuel kernel and 3) high-density graphite sphere. Fig. 3 shows sketches of each improved models and corresponding material properties.

Table 6-1 Constant used in 2D axial symmetric analysis

Defined Constant	Value	Descriptions
k_ss304	21.5[W/(m*K)]	Thermal conductivity of Stainless Steel 304
rho_ss304	8000[kg/m^3]	Density of Stainless Steel 304
cp_ss304	500[J/(kg*K)]	Heat Capacity at constant Pressure of SS 304
rho_neon	0.9002[g/liter]	Density of Neon
cp_neon	0.618[kJ/(kg*K)]	Heat Capacity at constant Pressure of Neon
k_graphite	25[W/(m*degC)]	Thermal conductivity of graphite
rho_graphite	1700[kg/m^3]	Density of graphite
cp_graphite	1.9[kJ/(kg*degC)]	Heat Capacity at constant Pressure of graphite
Q_pebble	1.23e8[W/m^3]	Average power generation of pebble
rho_shell	0.5[g/cm^3]	Density of low-density graphite shell
rho_kernel	1.74[g/cm^3]	Density of the fuel kernel region of the pebble
rho_core	60212572[g/cm^3]	Density of the pebble core graphite
temp_inlet	50[degC]	Inlet temperature
temp_RB	50[degC]	Temperature of the RB region, located outside the coolant
p	1[atm]	Pressure for Helium and Neon
v_water	2[m/s]	Velocity of the coolant
v_helium	5[m/s]	Velocity of Helium in the gas jacket
vmax_helium	8[m/s]	Maximum velocity of Helium in the gas jacket

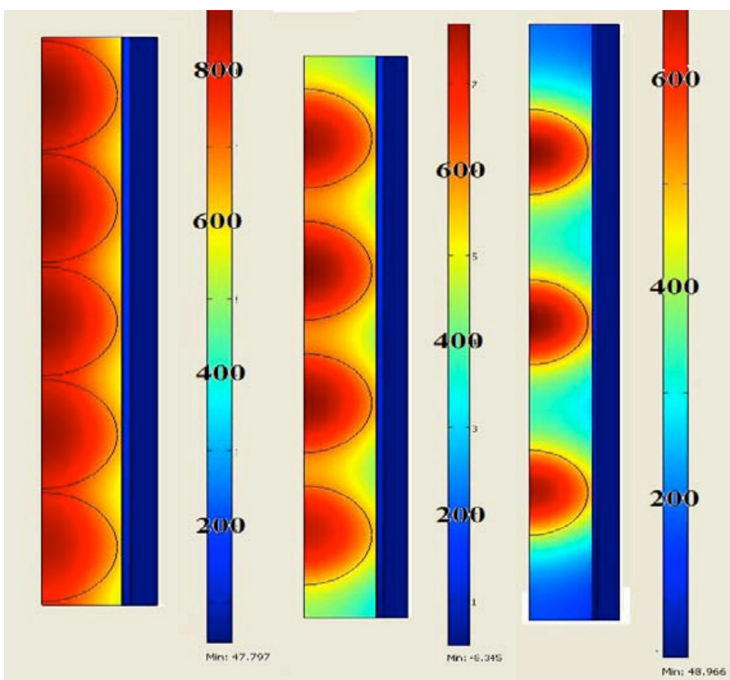

Fig. 6-1 Axial symmetric analysis on simplified 5 pebbles, 4 pebbles and 3 pebbles model

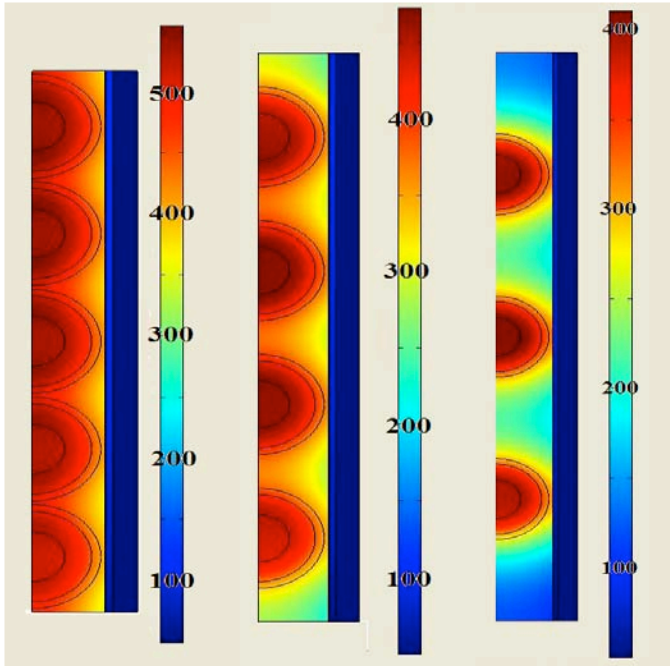

Fig. 6-2 Improved axial symmetric analysis on 5 pebbles, 4 pebbles and 3 pebbles models

Fig. 6-2 shows the temperature distribution of the improved pebble models. Although the maximum temperature drops around 300°C for each model, the distribution remains the same. Capsules' overall temperature distributions do not change much while the bottom of each capsule appears to be cooler. Making comparison between three different models, the 4 pebbles models remains to be the better choice out of the three: higher number of pebbles in single capsule with better temperature distribution.

All of the above thermal analysis consist only Helium in the gas jacket. However in the actual test reactor, Helium gas is mixed with Neon gas. Because two gases have different thermal properties, temperatures distribution among the capsule is likely to change depending on the mixing ratios. Therefore it is important to develop understandings of the effect of Neon gas has on the temperature. The next section will discuss the axial symmetric thermal analysis done with Neon filled gas jacket.

6.1.1 Neon Consideration

The usage of Helium and Neon gas in the gas jacket as mentioned in the earlier sections is to control and monitor temperature changes in the capsule. Thermal analysis in the last section with Helium filled gas jacket shows that temperature drops dramatically within the gas jacket; and regions outside the gas jacket remain at low temperature. The result confirmed that Helium gas is a good insulator that traps heat within the graphite spacer. With Neon replacing Helium, the thermal analysis that was done is shown below.

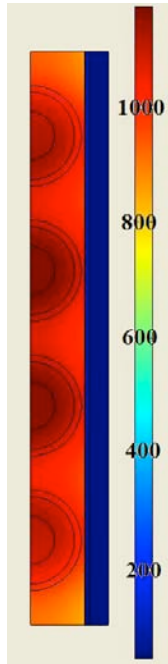

Fig. 6-3 Axial symmetric thermal analysis 4 pebbles model with Neon filled gas jacket

Thermal analysis with Neon filled gas jacket as done on with the 4 pebbles. The result in Fig. 12 shows that Neon is a better thermal insulator then Helium. This thermal analysis confirms the effects of Neon discussed in earlier sections.

Noting from the above thermal analysis, the temperature drops/increases significantly in the gas jacket region. Since Helium/Neon in the gas jacket is assumed to be stationary in the previous analysis, it is necessary to improve the model to get more accurate results in such region with dramatic temperature change. In the following subsection, Helium/Neon in the gas jacket is modelled considering gas flow.

6.1.2 Gas Jacket with flowing Helium/Neon

Although the 4 pebble model is favor over the other 2 models from previous analysis, there is no guarantee that the temperature distribution will remain the same. Therefore, thermal analysis will be done on all three models with Helium/Neon flowing in the gas jacket. However, the following assumptions still hold: 1) All pebbles have identical power generation; and 2) Simplified capsule geometry from actual capsule design. The flow rate of the Helium/Neon is calculated to 30cc/min.

There is no significant changes between the two temperature distributions between stationary Helium and flowing Helium. The maximum temperature difference between the models is differing by a factor of 10^{-1}. Close inspection on the temperature gradient shows no significant difference between the two models. This thermal analysis result shows that conduction is the dominant heat transfer path of Helium/Neon in the gas jacket and it is safe to assume the Helium/Neon in the gas jacket is stationary.

Based the previous thermal analysis, the 4 pebbles model appears to be the better option between three different models to continue to work on. In the next section, a better refined 2D, 4-pebble model will be examined.

6.2 Refined 2D Axial Symmetric Thermal Analysis

Thermal analysis simplified 2D geometry of the capsules provides a general temperature that helps determined the number of pebbles per capsules. However such model cannot further provide useful information that will aid the placement of the thermal couple due to the simplicity of the geometry. Refining the geometry that is more relevant to the actual design is essential to produce a better defined temperature distribution.

A refined 2D 4 pebbles geometry is shown where the graphite spacers are now covered by stainless steel caps on both the top and the bottom; additionally, a thin layer of Helium/Neon filled gas jacket exists in between the stainless steel cap and the graphite spacer. A thermal analysis is done on this 2D refined 4 pebble capsule model below.

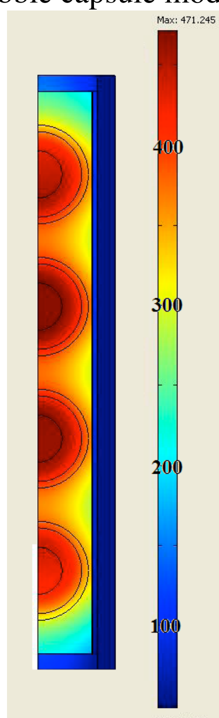

Fig. 6-3 Axial symmetric thermal analysis of refined 2D 4 pebbles geometry

The refined 4-pebble model shows a substantially uniform temperature distribution. With the addition of the stainless steel lid on the bottom and the gas jacket, the capsule that will be placed on the bottom of the test location shows significant improvement in terms of temperature distribution within the graphite spacer. This thermal analysis confirms the necessity of refining the geometry to receive a more precise model in comparison to the actual design.

7.0 CAPSULE SPECIFIC THERMAL ANALYSIS

The 2D y-z plane (axial symmetric) thermal analysis provides some useful insights which aids the selection of number of pebbles per capsules and gives conformation on designs' geometries such as space between pebbles, gas jacket thickness and coolant flow rate.

In order to acquire a better understanding on each of the capsule designs, 3D thermal analysis is preferred as it provides temperature distribution on both radial and axial directions on designs that are not axial symmetric. However, numbers of simulation errors had occurs in the course of 3D thermal analysis primary due to the fact that COMSOL™ lacks a powerful algorithm program and as a result 1) COMSOL™ fail to mesh CAD model imports because CAD models consist tiny faces (e.g. edges); 2) COMSOL™ failed to mesh small geometries even when the sketch has drawn on COMSOL™.

To replace the 3D thermal analysis, 2D x-y (radial) thermal analysis are performed instead on each of the following designs, while 2D y-z (axial symmetric) thermal analysis are done on some but not all due to limited information that can retrieved from the y-z analysis. Note that because of the unrealistic boundary condition, the temperature range on the radial thermal analysis is off by certain factor while the temperature distribution is still valid.

7.1 ATR3" 1 Pebble Capsule Design

The thermal analysis on the y-z plane of the ATR3" 1 pebble capsule design is essentially same as the thermal analysis done on 4 pebbles model in section 1.2, the only difference is the power generation of pebbles is now corresponding to pebble's position due to the axial flux variation within the test position. Thermal analysis is done on both radial and axial direction.

Since this capsule design is axial symmetric, an axial thermal analysis is sufficient. The purpose of running thermal analysis on both radial and axial direction on the ATR3" 1 pebble design was to determine the consistency of the radial thermal analysis in compare to the axial analysis. The temperature distribution on the radial direction closely resembles the one on axial direction while the maximum temperature is off by a 100°C. The result shows that the radial maximum temperature is not too far off from the axial temperature, in which case the x-y plane analysis can potentially provide some useful insights on other capsule design.

7.2 ATR3" 3 Pebble Capsule Design

Upon inspection of the ATR3" 3 pebble capsule design, pebbles are located very close to others and the design would appear to fail as the temperature of the pebbles and the graphite spacer will rise to temperature above the PB-AHTR maximum temperature. The y-z plane thermal analysis will not be useful because pebbles would appear to overlap each others.

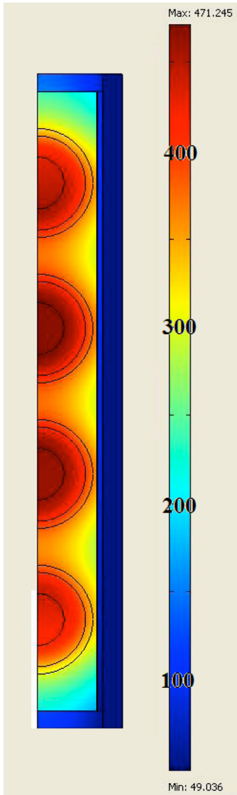

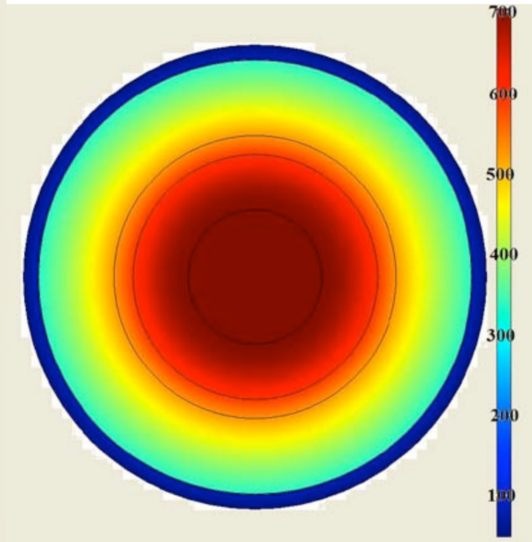

Fig. 7-1a Axial thermal analysis on ATR3” 1 pebble model
Fig. 7-1b Radial thermal analysis on ATR3” 1 pebble model

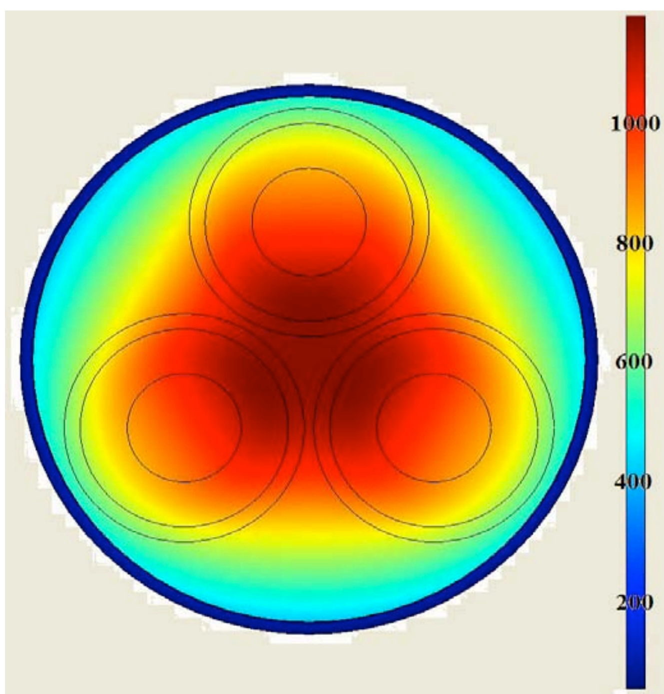

Fig. 7-2 Radial thermal analysis on ATR3” 3 pebble model

The radial thermal analysis on the ATR3” 3 pebble design reveals that the design is not sufficient to be test. The maximum temperature reaches as high as 1183°C, which is higher than the PB-AHTR temperature. Although the radial maximum temperature demonstrates by the analysis is slightly higher then the real time situation, a capsule design with maximum temperature over 1000°C is too risky and unsafe to use or test.

7.3 ATR5” 5 Pebble Capsule Design

The ATR5” 5 pebble design consists of five pebbles on each level. The larger test location allows the capsule design to fit more pebble in one level, yet have sufficient spacing between each pebble to prevent packing situation like ATR3” 3 pebble design. Thermal analysis of the ATR5” 5 pebble design on the x-y plane is shown below.

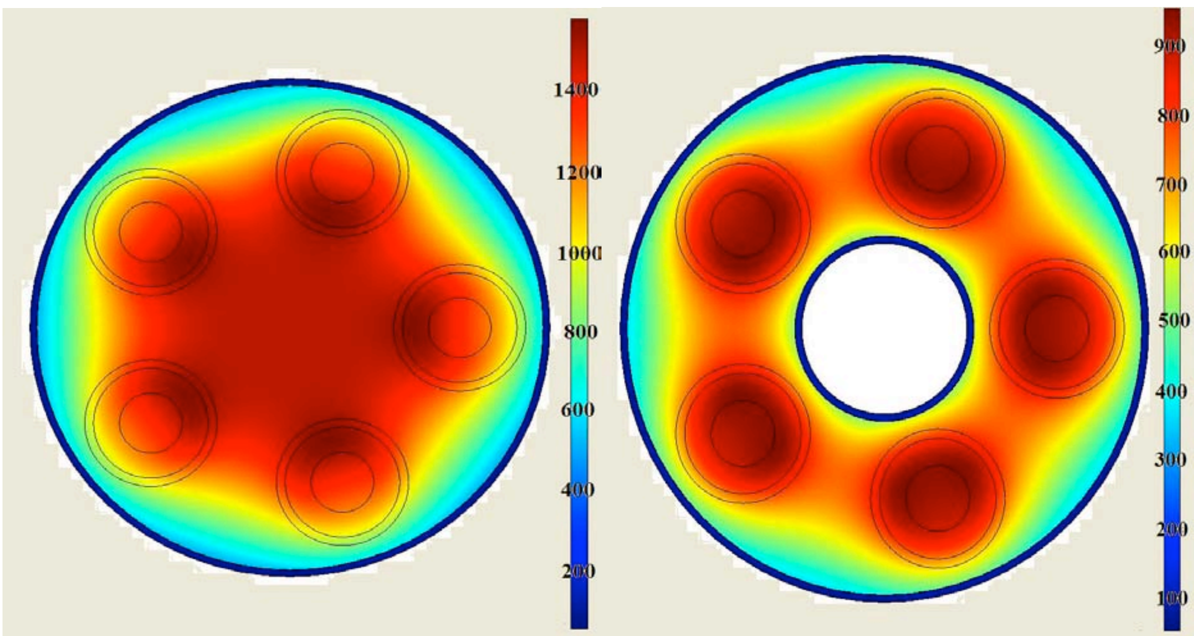

Fig. 7-3a Initial ATR5” 5 pebble capsule design
Fig. 7-3b Refined ATR5” 5 pebble design

The radial thermal analysis done on the initial ATR5” 5 pebble design results a high maximum temperature reaching 1599°C. With such high temperature, the design will not be useful for the same reason that the ATR3” 3 pebble design. Different from the ATR3” 3 pebble design, the ATR5” 5 pebble design has extra space to maneuver with. A line of coolant is added in the center of the design capsule so coolant with flow through and maximum temperature is expected to drops. The thermal analysis that is done on the refined ATR5” 5 pebble models shows maximum temperature drops from 1599°C to 952°C. Although temperature is still relatively high, the maximum temperature does drop significantly.

7.4 HFIR Capsule Design

The HFIR capsule design is similar geometrically to the ATR3” 1 pebble design. However, because HFIR is smaller compares to ATR and has a smaller test location, the geometry of the HFIR design is again constrained by the test location as mentioned in the earlier section. Like other designs, each of the two pebbles in the capsule has different power generation as they neutron flux vary axially. The thermal analysis of HFIR design is shown below.

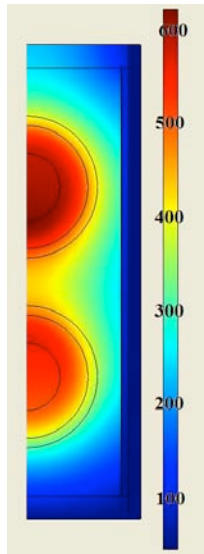

Fig. 7-4 Axial symmetric thermal analysis of HFIR capsule Design

Since the design is axial symmetric, only axial thermal analysis are done on the HFIR design and it shares similar temperature distribution with the ATR3” 1 pebble design, the fundamental difference between two design is number of pebbles per capsule.

8.0 SUMMARY

We have designed a set of test capsules that can be useful in qualifying high-temperature pebble fuels. Our designs' primary application is with the modular PB-AHTR effort, which is considering several potential fuel types including LEU fuel, deep burn TRU fuel, and thorium seed-blanket fuel. We have evaluated multiple test locations for PB-AHTR fuel testing in two U.S. test reactors, ATR and HFIR. The longer active core length and five-inch test locations make ATR a natural choice for testing pebbles en masse. There is some concern about the hard spectrum in these flux traps, which may result in irradiation damage of the pebble materials in excess of nominal PB-AHTR conditions. Future design work will incorporate shielding to tune the test reactor spectrum more precisely.

Preliminary COMSOL thermal analyses suggest that single-column test capsules create very uniform temperature profiles across the pebble surfaces. These capsules could be fielded in both ATR and HFIR. The three-column capsules designed for ATR's three-inch flux traps generated non-uniform temperature distributions that could not be remedied by 'short-circuiting' the heat flow with strips of copper. The five-column design for ATR's five-inch flux traps also resulted in a non-uniform temperature distribution that peaked on-axis, far above expected PB-AHTR operating temperatures. The inclusion of an additional coolant channel and gas jacket smoothed the temperature distribution and lowered the pebble temperatures closer to nominal conditions. This toroid design should provide a satisfactory testing environment for up to 60 pebbles simultaneously, reaching full burn-up in 0.9 years. This very rapid irradiation period is a major benefit of PB-AHTR's high power density operation, since it allows PB-AHTR fuel to be developed and qualified much more rapidly than conventional LWR, MHR, and SFR fuels.

9.0 REFERENCES

1. Philippe Bardet et al., "Design, Analysis and Development of the Modular PB-AHTR," Proceedings of ICAPP '08, Anaheim, CA USA, June 8-12, 2008
2. Per F. Peterson and Haihua Zhao, "Passive Decay Heat Removal for the Advanced High Temperature Reactor," Report UCBTH-03-005, U.C. Berkeley, February 12, 2004.
3. Petti, David. "An Overview of the DOE Advanced Gas Reactor Fuel Development and Qualification Program," ARWIF, February 2005.
4. Sterbentz, J. W. et al. "Reactor Physics Parametric and Depletion Studies in Support of TRISO Particle Fuel Specification for the Next Generation Nuclear Plant," INEEL/EXT-04-02331, September 2004.
5. Stanley, C. J. and Marshall, F. M. "Advanced Test Reactor – A National Scientific User Facility," INL/CON-07-13310, May 2008.
6. Thoms, K. R. et al. "HFIR Irradiation Facilities Improvements – Completion of the HIFI Project," *J. Nucl. Mat.* **155-157**, Part 2, pp. 1340-1345, 2 July 1988.
7. Grover, S. B. "Final Assembly and Initial Irradiation of the First Advanced Gas Reactor Fuel Development and Qualification Experiment in the Advanced Test Reactor," INL/CON-07-12136, May 2007.
8. K.R. Thoms and M.J. Kania, "Design, Fabrication, and Initial Operation of HTGR-ORR Capsule OF-2," Report ORNL-TM-5459, Oak Ridge Nat. Lab., 1977
9. Oak Ridge National Laboratory *Reactor Core Assembly* (n.d.) http://neutrons.ornl.gov/facilities/HFIR/
10. Mahmood, S T, "Neutron Dosimetry of the HFIR Hydraulic Facility," Report ORNL-TM-12831, Oak Ridge Nat. Lab., 1995
11. Cisneros, T., Greenspan, E., and Peterson, P. F. "Baseline Fuel Design for the Annular PB-AHTR," Report UCBTH-10-001, U.C. Berkeley, March 1, 2010.